INSTITUTE OF PHYSICS PUBLISHING JOURNAL OF PHYSICS: CONDENSED MATTER

J. Phys.: Condens. Matter **17** (2005) S975–S986 doi:10.1088/0953-8984/17/11/030

Novel phase diagram of superconductivity and ferromagnetism in UGe_2: a ^{73}Ge-NQR study under high pressure

Y Kitaoka[1], H Kotegawa[1,7], A Harada[1], S Kawasaki[1], Y Kawasaki[1,8], Y Haga[2], E Yamamoto[3], Y Ōnuki[2,3], K M Itoh[4], E E Haller[5] and H Harima[6]

[1] Department of Materials Engineering Science, Graduate School of Engineering Science, Osaka University, Toyonaka, Osaka 560-8531, Japan
[2] Advanced Science Research Center, Japan Atomic Energy Research Institute, Tokai, Ibaraki 319-1195, Japan
[3] Department of Physics, Graduate School of Science, Osaka University, Toyonaka, Osaka 560-0043, Japan
[4] Department of Applied Physics and Physico-Informatics, Keio University, Yokohama 223-8522, Japan
[5] Department of Materials Science and Engineering, University of California at Berkeley and Lawrence, Berkeley National Laboratory, Berkeley, CA 94720, USA
[6] Department of Physics, Faculty of Science, Kobe University, Nada, Kobe 657-8501, Japan

Received 5 January 2005
Published 4 March 2005
Online at stacks.iop.org/JPhysCM/17/S975

Abstract

We report on the pressure-induced novel phases of ferromagnetism (FM) and superconductivity (SC) in the itinerant ferromagnet UGe_2 through ^{73}Ge-NQR measurements under pressure (P). The P dependence of the NQR spectrum points to a first-order transition from strongly to weakly polarized ferromagnetic phases (SP and WP) around a critical pressure of $P_c^* \sim 1.2$ GPa. Furthermore, it shows the phase separation into the ferromagnetic and paramagnetic phases around $P_c \sim 1.6$ GPa. SC exhibiting a maximum value of the superconducting transition temperature $T_{sc} \sim 0.7$ K at $P_c^* \sim 1.2$ GPa was found to take place in connection with a P-induced first-order transition from SP to WP. The measurement of nuclear spin lattice relaxation rate $1/T_1$ has probed the ferromagnetic transition, exhibiting a peak at the Curie temperature as well as a decrease without the coherence peak below T_{sc}. These results reveal the uniformly coexistent phase of FM and unconventional SC with a line-node gap. Around P_c where the FM disappears, it is shown that SC occurs under the background of FM, but not in the paramagnetic phase. We remark on an intimate interplay between the onset of SC and the underlying electronic state for SP and WP.

[7] Present address: Department of Physics, Faculty of Science, Okayama University, Okayama 700-8530, Japan.
[8] Present address: Department of Physics, Faculty of Engineering, Tokushima University, Tokushima 770-8506, Japan.

1. Introduction

The coexistence of magnetism and superconductivity (SC) is one of the recent topics in condensed-matter physics. The uniformly coexistent phase of antiferromagnetism (AFM) and SC has been reported in UM_2Al_3 (M = Pd, Ni) [1], $CeCu_2Si_2$ [2–4], $CeIn_3$ [5–7], and $CeRhIn_5$ [8–10], where f-electrons are anticipated to contribute to both AFM and SC. Recently, in a ferromagnet UGe_2 with the Curie temperature $T_{\rm Curie} = 52$ K at ambient pressure ($P = 0$), P-induced SC was discovered to emerge under $P = 1$–1.6 GPa, exhibiting a highest transition temperature $T_{\rm sc} \sim 0.7$ K at $P_{\rm c}^* \sim 1.2$ GPa [11, 12]. It is noteworthy that the SC in UGe_2 disappears above $P_{\rm c} \sim 1.6$ GPa beyond which ferromagnetism (FM) is suppressed. This fact implies that the SC and the FM in this compound may be cooperative phenomena. It is, however, currently believed that the uniformly coexistent phase of FM and SC is unlikely to exist because the Cooper pairs feel a non-vanishing internal field to prevent the onset of a spin-singlet SC. It is, therefore, surprising that both FM and SC are carried by 5f electrons of uranium atoms and the SC coexists with the FM with a large moment of the order of 1 $\mu_{\rm B}$/U, which suggests that a spin-triplet pairing state may be formed. Although SC and FM have been reported in $HoMo_6S_8$ [13], $ErRh_4B_4$ [14] and $ErNi_2B_2C$ [15], note in these cases that $T_{\rm Curie} < T_{\rm sc}$ and the two orders are competing. The FM is carried by localized 4f electrons of Ho and Er atoms, whereas the SC is by conduction electrons. In this context, the recent discovery of SC in ferromagnets UGe_2 [11, 12], $ZrZn_2$ [16], and URhGe [17] has been a great surprise.

Figure 1 shows the pressure versus temperature (T) phase diagram of UGe_2 established from various measurements [11, 12, 18–21]. $T_{\rm Curie}$ decreases monotonically from $T_{\rm Curie} = 52$ K at $P = 0$ with increasing P. SC sets in at pressures exceeding $P \sim 1.0$ GPa, exhibiting a maximum value of superconducting transition temperature $T_{\rm sc} \sim 0.7$ K around $P_{\rm c}^* \sim 1.2$ GPa. The measurements of magnetization $M_{\rm s}(T)$ and resistivity show anomalous behaviours at T^* far below $T_{\rm Curie}$ [12, 20]. Since $M_{\rm s}(T)$ increases below T^* upon cooling, the low-T phase is denoted as a strongly polarized phase (SP) and the high-T one as a weakly polarized phase (WP) as indicated in the phase diagram. An interesting point is that the value of $T_{\rm sc} \sim 0.7$ K becomes maximum at $P_{\rm c}^* \sim 1.2$ GPa, where T^* disappears as if it were a termination point of a first-order transition from SP to WP [21]. The fact that both the SC and FM disappear simultaneously at $P_{\rm c} \sim 1.6$ GPa suggests that the SC is in a spin-triplet pairing state under the background of FM. However, it has been suspected from the measurements of diamagnetic susceptibility that both the phases do not coexist, but rather compete with each other; as P increases, a volume fraction of SC grows over the whole system, whereas the FM seems to become spatially inhomogeneous [22]. This result raises a question whether or not a uniformly coexistent phase of SC and FM is realized in UGe_2, if both of them are spatially homogeneous.

In this paper, we report on a series of nuclear-quadrupole-resonance (NQR) measurements of enriched ^{73}Ge that address the microscopic characteristics of SC and FM in UGe_2 [23]. What type of superconducting order parameter is realized in UGe_2 is also addressed.

2. Experimental details

A polycrystalline sample enriched in ^{73}Ge was prepared and crushed into powder for nuclear-quadrupole-resonance (NQR) measurements. Hydrostatic pressure was applied by utilizing a BeCu piston-cylinder cell, filled with Daphne oil (7373) as a pressure-transmitting medium. To calibrate the value of P at a sample position at low temperatures, the P-induced variation of $T_{\rm c}$ of Sn was measured by a high-frequency ac-χ measurement using an *in situ* NQR coil. Furthermore, in order to inspect the pressure gradient in the cell, we measured the P

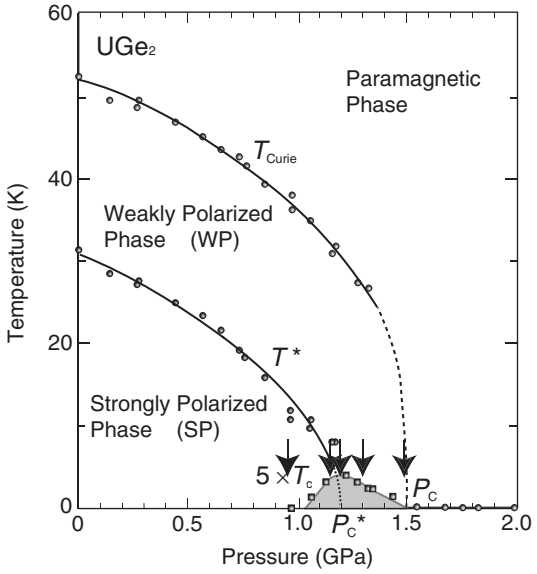

Figure 1. The pressure versus temperature phase diagram of UGe_2 [18, 19]. Arrows show values of P where the present NQR measurements have been made.

increasing rate $d\nu_Q/dp$ of the quadrupole frequency ν_Q of a reference sample ($CeCu_2Si_2$) with the narrowest linewidth ($\Delta\nu_Q \sim 0.01$ MHz) in the NQR spectrum to date. In this sample, as P increases, ν_Q increases linearly due to a linear increase of the electric field gradient at the Cu site that is caused by an increase in the lattice density. Using $d\nu_Q/dp = 9.52$ Hz bar^{-1}, a gradual increase of $\Delta\nu_Q$ with increasing P assures a distribution of P, $\Delta P/P$, of less than 3% in the cell for NQR measurements. A ^{3}He–^{4}He dilution refrigerator was used to reach the lowest temperature of ∼50 mK. The NQR experiment was performed by the conventional spin-echo method under zero field in the frequency (f) range of 5–12 MHz.

3. Microscopic evidence for the first-order transition

3.1. The phase separation into weakly and strongly polarized phases (WP and SP) around $P_c^* \sim 1.2$ GPa

Figure 2 shows the T dependence of the ^{73}Ge-NQR spectra at $P = 1.2$ GPa where T_{Curie} was decreased down to $T_{Curie} = 31$ K. In figure 2, the NQR spectrum (a) was measured at $T = 45$ K for the paramagnetic state, and the respective spectra of (b) and (c) at $T = 28$ and 4.2 K in the FM state. The spectrum (a) reveals a structure consisting of well separated peaks associated with three inequivalent Ge sites in a unit cell (see figure 2). A Ge1 site is closely located along a uranium (U)-zigzag chain. The other two Ge2 and Ge3 sites are out of this zigzag chain. The number of Ge1 sites is twice as large as the number of Ge2 and Ge3 sites in one unit cell. The respective values of the asymmetry parameter η of the electric field gradient (EFG) at the Ge1, Ge2 and Ge3 sites were calculated on the basis of band calculation by one of authors (Harima) to be $\eta = 0.95$, 0.68 and 0.72. Note that a ^{73}Ge-NQR spectrum with a nuclear spin of $I = 9/2$ consists of four equally separated peaks in the case of a symmetric EFG, whereas in the case of an asymmetric EFG, they are no longer equally separated. Instead, the four peaks collapse into two peaks. The two large peaks around 6 and 8.5 MHz in the

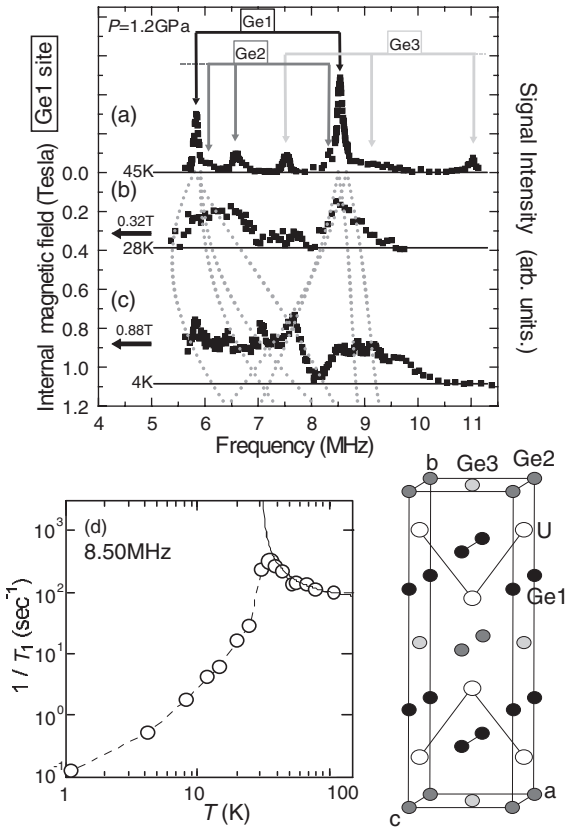

Figure 2. The temperature dependence of NQR spectra at $P_c^* = 1.2$ GPa. The NQR spectrum (a) at $T = 45$ K for the paramagnetic state reveals well separated peaks associated with three Ge sites (see the below right of figure 2). Note that, due to the asymmetry parameter $\eta \sim 1$ at the Ge1 site (see text), the NQR spectrum for the Ge1 site consists of two main peaks, whereas each spectrum at the Ge2 and Ge3 sites consists of four peaks, although the lowest and highest peaks for the Ge2 and Ge3 sites are out of the observation range. The respective NQR spectra (b) and (c), which were obtained at $T = 28$ and 4.2 K below $T_{\rm Curie} = 31$ K, are affected by the internal field ($H_{\rm int}$) induced by the onset of FM. The dotted lines trace the change in NQR frequencies caused by the increase in $H_{\rm int}$ upon cooling. (d) The T dependence of $1/T_1T$ at 8.50 MHz. The solid curve is a calculation based on the SCR spin-fluctuation theory for weakly itinerant ferromagnets [25]. The below right indicates the crystal structure of UGe_2.

NQR spectra (a) are assigned to the Ge1 site with the parameters of $\eta = 0.98$ and an NQR frequency $\nu_{\rm Q} \sim 2.3$ MHz, consistent with the calculation for the Ge1 site. The other peaks are by reason assigned to arise from the Ge2 and Ge3 sites as indicated in the figure, allowing us to deduce $\eta = 0.74$ and 0.80, although these values are somewhat larger than the calculated values $\eta = 0.68$ and 0.72, respectively. Thus, three Ge sites are separately noticed in the ^{73}Ge-NQR spectra observed in the range $f = 5$–12 MHz.

Below $T_{\rm Curie} = 31$ K at $P = 1.2$ GPa, the NQR spectra undergo a marked change upon cooling, as is seen in figures 2(b) and (c). This is because the onset of FM induces an $H_{\rm int}$ at the Ge sites causing Zeeman splitting in each of the Ge NQR spectra. Here, we focus on the change in the NQR spectra under the presence of $H_{\rm int}$ at the Ge1 site which is closely located to the uranium zigzag chain responsible for FM. In fact, the dotted curves in figure 2

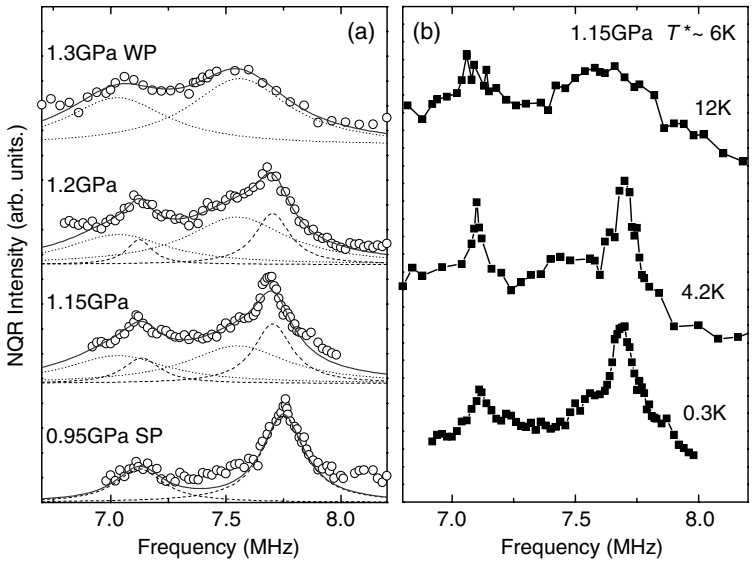

Figure 3. (a) The P dependence of the ^{73}Ge spectra at ∼0.3 K. The spectrum for WP (SP) at $P = 1.3$ (0.95) GPa is simulated by the overlap of two broad (sharp) Lorentzian spectra as indicated by dotted (dashed) curves. The spectra at $P = 1.15$ and 1.2 GPa are reproduced by the superposition of the sharp and broad two Lorentzian spectra for SP and WP, respectively, demonstrating that phase separation takes place. (b) The T dependence of the spectrum at $P = 1.15$ GPa. The sharp peak associated with SP appears suddenly below $T^* \sim 7$ K around which the transition from WP to SP is of first order.

trace the change in NQR frequencies as $H_{\rm int}$ increases at the Ge1 site upon cooling. The NQR spectra in figure 2(a), that consist of two peaks for the Ge1 site at the paramagnetic state, are split into multi-NQR lines. From the comparison between experiment and calculation, the respective values of $H_{\rm int} = 0.32$ and 0.88 T are tentatively estimated at $T = 28$ and 4.2 K for the Ge1 site. When noting that the NQR spectra for FM are seemingly observed around the same frequencies as those in the paramagnetic state, one may suspect that some non-magnetic sites remain separated spatially in the sample even below $T_{\rm Curie}$. In order to check this possibility on a microscopic level, the nuclear spin–lattice-relaxation rate $^{73}(1/T_1)$ was measured at $f = 8.50$ MHz where the NQR spectrum for the Ge1 site has its strongest peak in the paramagnetic state. As indicated in figure 2(d), a clear drop in $1/T_1$ below $T_{\rm Curie}$, associated with the depression of low-lying magnetic fluctuations, revealed that all the Ge sites in the sample are affected by the onset of FM. It is furthermore noteworthy that the T dependence of $1/T_1$ in the paramagnetic state obeys a relation of $T/(T - T_{\rm Curie})$ which is the T variation predicted by the self-consistently renormalized (SCR) spin-fluctuation theory for weakly itinerant ferromagnets [25].

Figure 3(a) indicates the P dependence of the spectrum in the $f = 7$–8 MHz range for the Ge1 site at $T = 0.3$ K for $P = 0.95$, 1.15, 1.2 and 1.3 GPa where SC emerges. The spectrum for WP at $P = 1.3$ GPa is significantly broader than that for SP at $P = 0.95$ GPa. Each spectrum is well simulated by taking into account the overlap of two Lorentzian spectra. Their full-width at a half maximum Δf is twice as large for WP ($\Delta f \sim 0.53$ MHz) than for SP ($\Delta f \sim 0.20$ MHz) as seen in figure 3(a). A remarkable finding is that the spectra at $P = 1.15$ and 1.2 GPa are reproduced by the superposition of the sharp (dashed curves) and broad (dotted curves) two Lorentzian spectra for SP and WP, respectively, demonstrating that

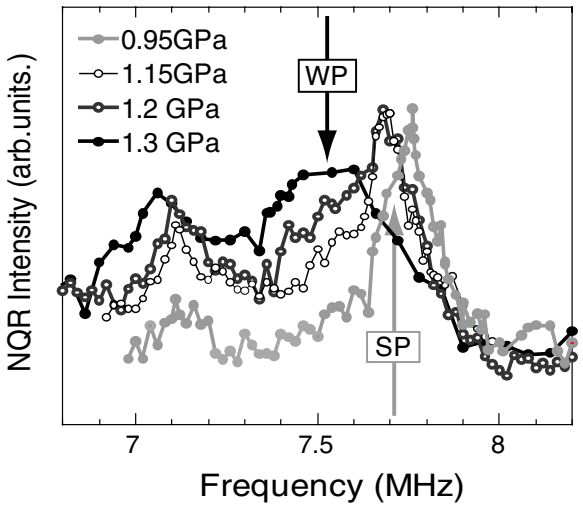

Figure 4. The P dependence of the ^{73}Ge spectra in the $f = 7$–8 MHz range at ∼0.3 K for $P = 0.95$, 1.15, 1.2 and 1.3 GPa.

phase separation takes place. Here, a fraction of SP to WP is estimated as SP:WP $= 5 \pm 1{:}5 \mp 1$ and $2 \pm 1{:}8 \mp 1$ at $P = 1.15$ and 1.2 GPa, respectively. This evidences that the P-induced magnetic transition from SP to WP is of first order, consistent with other measurements [21, 26]. However, a phase separation into SP and WP due to a pressure distribution of $\Delta P \sim 0.03$ GPa at P_c^* cannot be ruled out.

Figure 3(b) indicates the T dependence of the spectrum at $P = 1.15$ GPa where the transition temperature T^* from WP to SP is estimated as $T^* \sim 7$ K from other measurements [27]. The broad spectrum for WP at 12 K above T^* resembles that at $P = 1.3$ GPa and $T = 0.3$ K as seen in the top of figure 3(a). As seen in the spectrum at $T = 4.2$ K below $T^* \sim 7$ K, on the other hand, the sharp spectrum appears suddenly, associated with the first-order transition from WP to SP. The P dependence of the spectrum presented in figure 4 also ensures that the sharp spectrum appears in association with the first-order transition from WP to SP around $P_c^* \sim 1.2$ GPa. These results, therefore, suggest that the distribution of $H_{\rm int}$ for WP is smaller than that for SP, leading to the increase in magnetization for SP below T^*.

It should be noted that even though both WP and SP are separated around $P_c^* \leqslant 1.2$ GPa, the SC reveals the highest value of $T_{\rm sc} = 0.7$ K and as yet $T_{\rm sc}$ goes down at $P = 0.95$ and 1.3 GPa where SP and WP emerge without any trace of phase separation, respectively.

3.2. The phase separation into ferromagnetic and paramagnetic phases around $P_c \sim 1.6$ GPa

Figure 5(a) indicates the spectra for the paramagnetic phase at the region $T = 35$ K and $P = 1.5$ GPa close to $P_c \sim 1.6$ GPa where FM disappears. The spectra in the $f = 8.2$–8.8 MHz range arise from the Ge1 and Ge2 sites (see the spectra at 45 K in figure 2). Here, note that the two NQR lines for the Ge1 site are almost overlapped due to the asymmetry parameter $\eta \sim 1$. As the temperature decreases below 10 K, the spectral shape is slightly broadened, as is seen for the spectra at $T = 4.2$ K in figure 5(b), although the overall shape remains unchanged, suggesting that the system remains mostly in the paramagnetic state. This result reveals that there possibly occurs a phase separation into paramagnetic and ferromagnetic phases. Here,

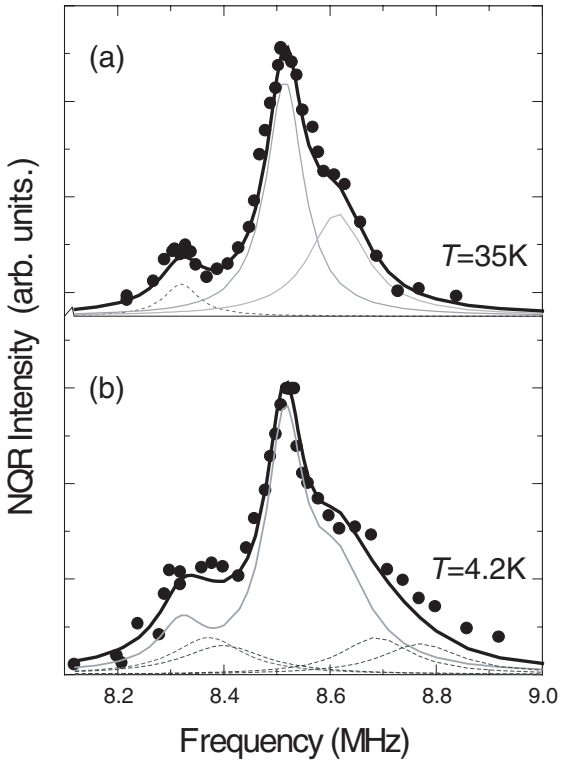

Figure 5. (a) The ^{73}Ge spectra at $T = 35$ K and $P = 1.5$ GPa in the paramagnetic phase. The spectrum in the range $f = 8.2$–8.8 MHz consists of two NQR transitions for the Ge1 site and one NQR transition for the Ge2 site. (b) The ^{73}Ge spectrum at $T = 4.2$ K where the phase separation into paramagnetic and ferromagnetic phases occurs. The spectrum is well simulated by assuming that the phase separation into paramagnetic and ferromagnetic phases exists with a ratio of 5:2 and $H_{\rm int} = 0.2$ T.

we focus on the change in the NQR spectrum under the presence of $H_{\rm int}$ at the Ge1 site due to the onset of FM. This is because the Ge1 site is closely located to the uranium zigzag chain responsible for the FM and then the number of Ge1 sites is twice as large as the number of Ge2 and Ge3 sites in one unit cell. In fact, the NQR spectrum that consists of two peaks for the Ge1 site at the paramagnetic state in figure 5(a) splits into multi-NQR lines due to the appearance of $H_{\rm int}$ at the Ge1 sites as indicated by the solid curves in figure 5(b). From the comparison between experiment and calculation, the ratio of the paramagnetic to ferromagnetic phase is estimated to be 5:2 and the internal field at the Ge1 site as $H_{\rm int} = 0.2$ T at $T = 4.2$ K. Thus, a first-order transition from ferromagnetic to paramagnetic phase was evidenced from the microscopic point of view. Recent T_1 measurements have revealed that SC sets in the ferromagnetic phase at $T_{\rm sc} \sim 0.2$ K, but it does not in the paramagnetic phase [24].

4. Evidence for unconventional superconductivity

Next we move on to the superconducting characteristics of UGe_2. Figures 6(a) and (b) indicate the T dependence of $1/T_1$ measured at the NQR peak at $f = 7.75$ MHz for the spectrum at $P = 1.15$ and 1.2 GPa where SP and WP are separated. Note that $1/T_1$ is uniquely determined; nevertheless, the peak arises from both SP and WP with a comparable fraction, as seen in

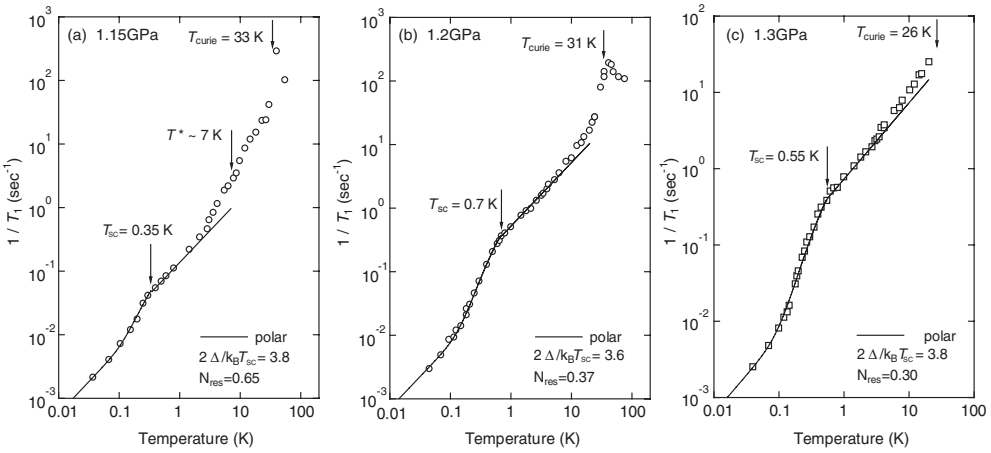

Figure 6. The T dependence of $1/T_1$ at (a): $P = 1.15$ GPa and (b) 1.2 GPa measured at the peak at $f = 7.75$ MHz. The identification of both the phase transitions into SC and FM ensures their uniformly coexistent phase. (c) The T dependence of $1/T_1$ at $P = 1.3$ GPa measured at the peak in the spectrum for WP. The solid curve in each panel is a calculation based on an unconventional superconducting model with a line-node gap (see the text).

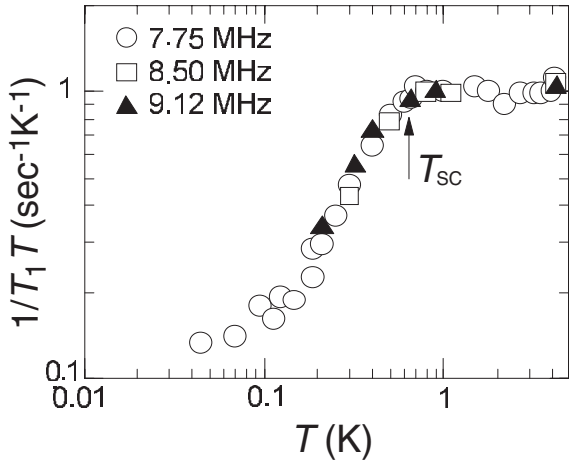

Figure 7. The frequency dependence of $1/T_1T$ at $P_c^* = 1.2$ GPa in the range $f = 7.75$, 8.5 and 9.12 MHz. The observation of a similar T dependence of $1/T_1T$ ensures the onset of SC over the whole sample.

figure 3(a). Figure 6(c) measured at the peak for the spectrum for WP at $P = 1.3$ GPa does that as well. The T_1 measurements probe the SC at $T_{sc} = 0.35$, 0.7, and 0.55 K (± 0.05 K) for $P = 1.15$, 1.2, and 1.3 GPa, respectively. In order to confirm the bulk nature of the SC for both the phases, $1/T_1T$ at $P = 1.2$ GPa was measured in the range $f = 7.75$, 8.5 and 9.12 MHz. As indicated in figure 7, all the data reveal a similar T dependence across T_{sc}, supporting the homogeneous and bulk nature of SC on a microscopic level. $1/T_1$ reveals a rapid decrease below T_{Curie}, followed by a $T_1T \sim$ constant-like behaviour upon cooling. In the superconducting state, a clear decrease in $1/T_1$ is evident below T_{sc}. Thus, the T_1 result, which probes both the transitions into FM and SC, evidences that SC coexists with both SP

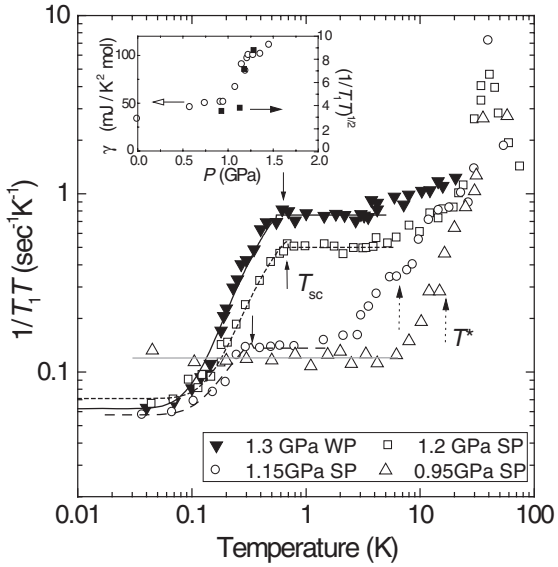

Figure 8. The T dependence of $1/T_1T$. At $P = 1.15$ and 0.95 GPa, $1/T_1T$ decreases for SP below around T^*. The value of $1/T_1T$ for WP is significantly larger than those for SP. The inset indicates that the P dependence of $(1/T_1T)^{1/2}$ (squares) scales to that of the T-linear electronic contribution in specific heat γ (circles). The data of γ are taken from [20].

and WP on a microscopic level. Markedly, $1/T_1$ decreases without any signature of coherence peak just below T_{sc}, which gives evidence for an unconventional nature of SC. In fact, the data of $1/T_1$ are well fitted by an unconventional superconducting model with line-node gap that assumes a residual density of states (DOS) N_{res} at the Fermi level. As indicated by solid curves in figures 6(a)–(c), the magnitude of the superconducting energy gap Δ and N_{res} are estimated to be $2\Delta/k_BT_{sc} \sim 3.8$, 3.6 and 3.6, and $N_{res} = 0.65$, 0.37 and 0.30 at $P = 1.15$, 1.2 and 1.3 GPa, respectively. In this model, the origin of N_{res} cannot be ascribed due to some impurity effect, because N_{res} depends on the value of P. In the non-unitary odd-parity pairing model [28, 29], the unique relaxation behaviour is predicted to depend on the angle between the quantization axis of the nuclear-spin system and that of the electron-spin one in the non-unitary odd-parity (spin-triplet) SC [30]. When the former axis is parallel to the latter one, the behaviour of $1/T_1 \sim T^2$ is expected at low T, which is inconsistent with the behaviour of $1/T_1 \sim T^{2.2}$ below T_{sc} at $P_c^* \sim 1.2$ GPa. At the present stage, however, since the angle between the quantization axis of the nuclear-spin system and that of the electron-spin one cannot be deduced experimentally, further analysis on the basis of this model is not yet possible. From a different point of view, it should be noted that the value of $1/T_1T$ retains nearly the same magnitude well below T_{sc}, independent of P. It is likely that this result in UGe_2 is relevant to either the gapless low-lying quasiparticle excitations inherent to the uniformly coexistent phase of FM and SC or the presence of a self-induced vortex core which may be responsible for this relaxation process.

5. Evidence for an underlying difference in the electronic state of strongly and weakly polarized ferromagnetic phases

In figure 8, $1/T_1T$ versus T plots are presented at $P = 0.95$, 1.15, 1.2 and 1.3 GPa. All the data of $1/T_1$ show a $T_1T =$ constant behaviour down to T_{sc} far below T_{Curie}. The T_1

measurements probe the SC at $T_{sc} = 0.35$, 0.7, and 0.55 K (± 0.05 K) for $P = 1.15$, 1.2, and 1.3 GPa, respectively. The onset of SC was not confirmed down to ~50 mK at $P = 0.95$ GPa. A notable point is that the values of $1/T_1T$ above T_{sc} at $P = 1.3$ and 1.2 GPa are larger than the values at $P = 1.15$ and 0.95 GPa. The underlying electronic state in WP seems to possess a larger DOS than in SP. The value of $(1/T_1T)^{1/2}$ is proportional to the DOS at the Fermi level; in fact, the P dependence of $(1/T_1T)^{1/2}$ scales to that of the T-linear coefficient γ in specific heat at low T [27], as indicated in the inset of figure 8. This underlying electronic state behind the onset of SC is shown to make low-lying excitations enhance at the Fermi level near $P_c^* \leqslant 1.2$ GPa. As a matter of fact, once the value of P decreases even slightly from 1.2 to 1.15 GPa, T_{sc} decreases dramatically from $T_{sc} \sim 0.7$ K down to 0.35 K. Note that this value of $T_{sc} \sim 0.35$ K is significantly lower than $T_{sc} \sim 0.6$–0.7 K expected from other measurements. From the fact that SP makes the NQR peak larger around $f = 7.75$ MHz and its DOS is actually reduced, *it is likely that the SC for SP sets in at* $T_{sc} \sim 0.35$ K, *whereas the SC for WP does so at* $T_{sc} \sim 0.6$–0.7 K. Therefore, when the phase separation into SP and WP takes place just below P_c^*, it is considered that the superconducting nature differs at SP and WP exhibiting the SC at $T_{sc} = 0.35$ and 0.6–0.7 K, respectively. In this context, a reason why T_{sc} becomes a maximum at $P_c^* \leqslant 1.2$ GPa is that $T_{sc} = 0.7$ K coincides for both the phases regardless of the phase separation actually existing.

Finally, we wish to remark why SC emerges around the critical point for the first-order transition from SP to WP around $P_c^* \sim 1.2$ GPa. These new phenomena observed in UGe_2 should be understood in terms of first-order quantum phase transitions at which the system may fluctuate between states that are separated by a potential barrier. In fermion systems, if the magnetic critical temperature T^* is suppressed at P_c^*, it involves the diverging magnetic density fluctuations inherent at the critical point from SP to WP in the quantum Fermi degeneracy region. The Fermi degeneracy by itself generates various instabilities noted as Fermi surface effects, one of which is a superconducting transition. On the basis of a general argument on quantum criticality, it is shown that the coexistence of the Fermi degeneracy and the critical density fluctuations yields a new type of quantum criticality [31]. This makes the physics of first-order quantum phase transitions an extremely rich challenge in both theoretical and experimental studies.

From another context, it is predicted that T^* is identified with the formation of a simultaneous charge and spin density wave (CSDW), and hence near the critical point of this transition the superconducting pairing is mediated by CSDW fluctuations [32]. Extensive neutron diffraction studies, however, did not succeed in detecting any static order due to a CSDW, and also, the present NQR experiment did not provide possible evidence for the onset of CSDW below T^*. The results on UGe_2 deserve further theoretical investigations.

6. Summary

The ^{73}Ge-NQR measurements in UGe_2 have revealed the bulk nature of the SC which coexists with FM on a microscopic level. The P dependence of the NQR spectrum has revealed that the P-induced magnetic transition is of first order around $P_c^* \sim 1.2$ GPa, showing that a quantum critical point does not exist around P_c^*. The phases at $P = 1.15$ and 1.2 GPa are separated into SP and WP in association with an inevitable P distribution $\Delta P \sim 0.03$ GPa in the cell because 1.15 GPa $< P_c^* \leqslant 1.2$ GPa. Even so, it is demonstrated that the SC with the maximum value of $T_{sc} \sim 0.7$ K takes place under the background of such a phase separation.

The T dependence of $1/T_1$ below T_{sc} has been found to be well fitted by the line-node gap model with the N_{res} at the Fermi level. The large P dependence of N_{res} cannot be ascribed to some impurity effect. If the presence of a self-induced vortex state were responsible for

the T_1T = const well below T_{sc}, the P-induced variation in the DOS at the normal state should cause the P dependence of T_1T = const below T_{sc}. This was not the case. Further experiments are required for understanding the novel superconducting characteristics and for addressing a possible order parameter symmetry in UGe_2, either a unitary- or a non-unitary spin-triplet pairing state. Around P_c where the FM disappears, it is shown that SC occurs under the background of FM, but not in the paramagnetic phase.

Acknowledgments

The authors wish to thank K Machida, N Tateiwa, T C Kobayashi, G-q Zheng, A D Huxley and J Flouquet for helpful discussions. This work was supported by Grant-in-Aid for Creative Scientific Research (15GS0213), MEXT and the 21st Century COE Program supported by Japan Society for the Promotion of Science. HK and SK have been supported by Research Fellowship of the Japan Society for the Promotion of Science for Young Scientists.

References

[1] Geibel C *et al* 1991 *Z. Phys.* B **83** 305
Geibel C *et al* 1991 *Z. Phys.* B **84** 1
[2] Kitaoka Y, Ishida K, Kawasaki Y, Trovarelli O, Geibel C and Steglich F 2001 *J. Phys.: Condens. Matter* **13** L79–88
[3] Kawasaki Y, Ishida K, Mito T, Thessieu C, Zheng G-q, Kitaoka Y, Geibel C and Steglich F 2001 *Phys. Rev.* B **63** 140501(R)
[4] Kawasaki Y, Ishida K, Mito T, Zheng G-q, Kitaoka Y, Geibel C and Steglich F 2004 *J. Phys. Soc. Japan* **73** 194
[5] Mathur N D, Grosche F M, Julian S R, Walker I R, Freye D M, Haselwimmer R K W and Lonzarich G G 1998 *Nature* **394** 39
[6] Kawasaki S *et al* 2002 *Phys. Rev.* B **65** 020504(R)
[7] Kawasaki S, Mito T, Kawasaki Y, Kotegawa H, Zheng G-q, Kitaoka Y, Shihido H, Araki S, Settai R and Ōnuki Y 2004 *J. Phys. Soc. Japan* **73** 1647
[8] Hegger H, Petrovic C, Moshopoulou E G, Hundley M F, Sarrao J L, Fisk Z and Thompson J D 2000 *Phys. Rev. Lett.* **84** 4986
[9] Mito T, Kawasaki S, Kawasaki Y, Zheng G-q, Kitaoka Y, Aoki D, Haga Y and Ōnuki Y 2003 *Phys. Rev. Lett.* **90** 077004
[10] Kawasaki S, Mito T, Kawasaki Y, Zheng G-q, Kitaoka Y, Aoki D, Haga Y and Ōnuki Y 2003 *Phys. Rev. Lett.* **91** 137001
[11] Saxena S S *et al* 2000 *Nature* **406** 587
[12] Huxley A D, Sheikin I, Ressouche E, Kernavanois N, Braithwaite D, Calemczuk R and Flouquet J 2001 *Phys. Rev.* B **63** 144519
[13] Ishikawa M and Fischer Ø 1977 *Solid State Commun.* **23** 37
[14] Moncton D E, McWahn D B, Schmidt P H, Shirane G, Thomlinson W, Maple M B, MacKay H B, Woolf L D, Fisk Z and Johnston D C 1980 *Phys. Rev. Lett.* **45** 2060
Fertig W A, Johnston D C, DeLong E, McCallum R W, Maple M B and Matthias B T 1977 *Phys. Rev. Lett.* **38** 987
[15] Canfield P C, Bud'ko S L and Cho B K 1996 *Physica* C **262** 249
[16] Pfleiderer C, Uhlarz M, Hayden S M, Vollmer R, Löhneysen H v, Bernhoeft N R and Lonzarich G G 2001 *Nature* **412** 58
[17] Aoki D, Huxley A, Ressouche E, Braithwaite D, Flouquet J, Brison J-P, Lhotel E and Paulsen C 2001 *Nature* **413** 613
[18] Kobayashi T C, Hanazono K, Tateiwa N, Amaya K, Haga Y, Settai R and Ōnuki Y 2002 *J. Phys.: Condens. Matter* **14** 10779
[19] Haga Y, Nakashima M, Settai R, Ikeda S, Okubo T, Araki S, Kobayashi T C, Tateiwa N and Ōnuki Y 2002 *J. Phys.: Condens. Matter* **14** L125
[20] Tateiwa N *et al* 2001 *J. Phys. Soc. Japan* **70** 2876
[21] Pfleiderer C and Huxley A D 2002 *Phys. Rev. Lett.* **89** 147005
[22] Motoyama G, Nakamura S, Kadoya H, Nishioka T and Sato N K 2001 *Phys. Rev.* B **65** 020510(R)

[23] Kotegawa H *et al* 2003 *J. Phys.: Condens. Matter* **15** S2043
Kotegawa H, Harada A, Kawasaki S, Kawasaki Y, Kitaoka Y, Yamamoto E, Haga Y, Ōnuki Y, Itoh K M and Haller E E 2005 *J. Phys. Soc. Japan* at press
[24] Harada A *et al* 2004 unpublished
[25] Moriya T 1991 *J. Magn. Magn. Mater.* **100** 261
[26] Settai R, Nakashima M, Araki S, Haga Y, Kobayashi T C, Tateiwa N, Yamagami H and Ōnuki Y 2002 *J. Phys.: Condens. Matter* **14** L29
[27] Tateiwa N, Kobayashi T C, Hanazono K, Amaya K, Haga Y, Settai R and Ōnuki Y 2001 *J. Phys.: Condens. Matter* **13** L17
[28] Machida K and Ohmi T 2001 *Phys. Rev. Lett.* **86** 850
[29] Fomin I A 2001 *JETP Lett.* **74** 111
[30] Ohmi T and Machida K 1993 *Phys. Rev. Lett.* **71** 625
[31] Imada M 2004 *J. Phys. Soc. Japan* **73** 1851
[32] Watanabe S and Miyake K 2002 *J. Phys. Soc. Japan* **71** 2489